Endocrine, *vol. 29, no. 2, 299–307, April 2006* 0969–711X/06/29:299–307/$30.00
ENDO (Online) ISSN 1559-0100

Effects of Long-Term Adrenalectomy on Apoptosis and Neuroprotection in the Rat Hippocampus

Sergio Andrés,[1,*] Sergio Cárdenas,[1,*] Claudio Parra,[2] Javier Bravo,[1]
Monika Greiner,[1] Paulina Rojas,[1] Paola Morales,[3] Hernán Lara,[1] and Jenny Fiedler[1]

[1]Laboratory of Neurobiochemistry, Department of Biochemistry and Molecular Biology, Faculty of Chemical and Pharmaceutical Sciences, Universidad de Chile, P.O. Box 233, Santiago 1, Chile; [2]Physics Department, Iberoamerican University of Science and Technology, P.O. Box 13901, Santiago, Chile; and [3]Program of Molecular and Clinical Pharmacology, ICBM, Medical Faculty, University of Chile, P.O. Box 7000, Santiago 7, Chile

Reduction in corticosterone by acute adrenalectomy (5 d) promotes apoptosis in dentate gyrus (DG) granular neurons, an effect concomitant with variations in the expression of the *Bcl-2* gene family implicated in apoptotic regulation. However, no studies exist correlating the effect of long-term adrenalectomy (30 d) on the hippocampus in terms of extent of apoptosis and the levels of proteins related to an apoptotic cascade. After 5 d of adrenalectomy, we found an increase in apoptosis of the DG granular region, correlated with an increase in the processing of caspase-9. The magnitude of apoptosis 30 d after adrenalectomy was reduced in the DG granular layer compared with 5 d after adrenalectomy, in close relation to a reduction in the level of processed caspase-9. To understand how the increase in cell survival long after adrenalectomy occurs, we analyzed changes in the expression of genes and proteins related to apoptosis. Long-term adrenalectomy did not change hippocampal pro-apoptotic *Bax* or anti-apoptotic *Bcl-2* mRNA levels or protein content with respect to control. However, we found an increase in mRNA levels of the GD's *Bcl-x* gene, in parallel with the increase in anti-apoptotic BCL-X_L protein levels. These results suggest the reduction in apoptosis observed after long-term adrenalectomy occurs through mechanisms that repress proapoptotic genes previously found to be increased at shorter times of adrenalectomy.

Key Words: Adrenalectomy; corticosterone; apoptosis; BAX; BCL-X_L; BCL-2; BAD.

Introduction

Adrenal corticoids are known to influence neuronal function *(1,2)* and survival in the hippocampus *(3)*, a brain structure involved in learning and memory processes *(4)*. Several investigations *(5–8)* including our studies *(9)* have demonstrated that adrenalectomy (ADX) induces apoptosis in the granule cells of the dentate gyrus (DG), an effect prevented by corticosterone replacement, suggesting a trophic role for this hormone *(5,6,8,9)*. Molecular studies in the hippocampus have shown that cell death of granular neurons found 5 d after (i.e., short-term) ADX is associated with changes in the expression of the *Bcl-2* gene family, which regulates the apoptotic process *(9,10)*. We reported that *Bax*, *Bcl-2*, and *Bcl-x* mRNAs are topographically distributed within the hippocampus, and that their expression is modified by ADX and/or corticosterone administration *(10)*. Thus, 5 d after ADX, there was a significant increase in *Bax* mRNA levels and in *Bcl-2* mRNA levels in the suprapyramidal layer of the DG, effects prevented by corticosterone replacement.

Because in adult rats ADX increases both the proliferation rate of granular cell progenitors present in the subgranular zone in the hippocampus and the number of cells displaying apoptosis in the GD granular cell layer, it has been assumed that corticoids have a dual effect—one that inhibits cell proliferation and the other that has a trophic influence on granular cell survival *(3,5,6,8,11–13)*. It is therefore important to identify the corticoid-controlled pathways that are involved in neurogenesis and death. During the early events of apoptosis, mitochondria have been found to play a central role in programmed cell death *(14,15)*. Some apoptotic signal causing mitochondrial membrane permeabilization induces apoptosis in a process regulated by BCL-2-related proteins *(14)*, which control the release of mitochondrial cytochrome *c (15–17)*. On the other hand, the up-regulation of *Bax*, may explain the apoptosis observed in DG after short-term ADX (5 days after ADX), while *Bcl-2* induction may correspond to a compensatory mechanism protecting the cells from death *(10)*. Thus, the molecular effect of corticoids in the reduction of cell survival could depend on

Received October 14, 2005; Revised November 9, 2005; Accepted November 29, 2005.

Author to whom all correspondence and reprint requests should be addressed: Dr. J. L. Fiedler, Department of Biochemistry and Molecular Biology, Faculty of Chemical and Pharmaceutical Sciences, Universidad de Chile, P.O. Box 233, Santiago 1, Chile. E-mail jfiedler@ciq.uchile.cl

*Both authors contributed equally to the paper.

how different signal transduction pathways related to apoptosis, change with hormonal status. Interestingly, long-term deprivation of corticosterone (30 d post ADX) does not produce a loss of the entire DG which suggests: a) that the presence of additional sources of steroids could prevent neuronal loss *(18)* or b) long-term ADX may induce neuroplastic changes in the hippocampus, reducing the magnitude of apoptosis. The main focus of this paper is to demonstrate that some genes and proteins related to the *Bcl-2* family change during long-term ADX, modulating the cell death promoted by this experimental condition and explaining the viability of the hippocampal granular cell layer.

Results

Morphological Analysis of Apoptotic Granule Cells After Short- and Long-Term ADX

After short-term ADX (5 d after ADX) and long-term of ADX (30 d after ADX), corticosterone serum levels were reduced significantly (0.32 ± 0.2 μg/dL and 1.49 ± 0.24 μg/dL, respectively) compared to controls (13.86 ± 2.59 μg/dL). Dying cells were distinguished from healthy ones based on their apoptotic morphology after staining with Cresyl Violet. Three morphological profiles characteristic of apoptotic cells were observed, including a pyknotic nucleus, nuclei containing clumped chromatin disassembling into smaller particles, and a degenerating nucleus *(9)*. All of these profiles were included as apoptotic cells while counting.

Figure 1A reveals that the number of apoptotic cells in the hippocampus found 5 d after ADX were mainly present in the CA1 subfield and in both suprapyramidal and infrapyramidal blades of the DG considering cells present in both the mature granular layer and subgranular area. In contrast, after long-term ADX (30 d), we observed a decreased number of apoptotic cells present in CA1 and also in both layers of the DG compared to 5 d after ADX. Figure 1B demonstrates that the reduction observed in the number of apoptotic cells under long-term ADX was mainly due to a decrease in the number of apoptotic cells found in the mature granular cell layer of DG. However, both 5 and 30 d after ADX we observed a similar number of apoptotic cells in the subgranular zone of the DG (Fig. 1B).

Changes in the Active Form of Caspase-9 Immunoreactivity After Adrenalectomy

Upon apoptotic stimulation, cytochrome *c* is released from mitochondria and associates with procaspase-9 and Apaf 1 forming the apoptosome complex, with subsequent autoprocessing of procaspase-9 into its two active fragments (38-kDa and a 40-kDa prodomain) and a 17-kDa fragment *(15,19,20)*. We used a polyclonal antibody that recognizes the procaspase-9 (51 kDa) and the fragments generated by its cleaveage (Fig. 2A). Figure 2B shows that short-term ADX induces a significant increase ($p < 0.05$) in the active fragment of 38-kDa processed caspase-9 in contrast to the significant reduction ($p < 0.05$) observed under long-term ADX with respect to sham controls.

We also studied the caspase-3 activation, which is considered to be one of the major primary and irreversible steps in the apoptotic process mediating the proteolytic cleavage of many nuclear and cytosolic proteins *(20)*. Caspase-3 exists as an inactive zymogen (35 kDa) and is activated by initiator caspases that cleave the zymogen into active 17- and 19-kDa fragments *(20)*. We used a polyclonal antibody that detects both fragments in our immuno blotting analysis and observed the presence of the active form of caspase-3 (17-kDa) and the 19-kDa fragment both in sham and ADX animals (Fig. 2A). When data were expressed as a ratio between the 19-kDa active fragment and procaspase-3 (35 kDa), we did not observe an increase in the processed caspase-3 5 d after ADX. However, a significant increase of the active form of caspase-3 was observed 30 d after ADX (Fig. 2B).

Changes in mRNA Levels of Genes Regulating Cell Death 30 d After ADX

To determine whether long-term ADX promotes changes in the *Bcl-2* family mRNA similar to that observed previously 5 d after ADX, we measured the changes in *Bax*, *Bcl-2*, and *Bcl-x* mRNA level by *in situ* hybridization. As shown in Fig. 3A, 30 d after ADX the pro-apoptotic *Bax* mRNA levels were similar to sham-operated animals in every hippocampal subfield studied. Also, ADX did not change the steady-state level of anti-apoptotic *Bcl-2* mRNA in any region of the hippocampus (Fig. 3B). The *Bcl-x* gene generates long and short transcripts, which encode two proteins with anti-apoptotic ($BCL\text{-}X_L$) and pro-apoptotic ($BCL\text{-}X_S$) activity, respectively *(21,22)*. Considering that the riboprobe used in this study hybridizes both transcripts and owing to the relative abundance of the long transcript in whole hippocampus *(9)*, the hybridization observed probably represents this transcript. After 30 d of ADX, there is an approx 100% increase ($p < 0.05$) in *Bcl-x* mRNA in the supra- and infrapyramidal blade of DG (Fig. 3C).

Effect of Long-Term ADX on Pro- and Anti-apoptotic Protein Levels

Immunoblot analyses were used to examine whether the levels of *Bcl-x*, *Bcl-2*, and *Bax* mRNA correlated with their protein levels. Figure 4A shows a representative immunoblot for $BCL\text{-}X_L$, BCL-2, BAD, phospho-BAD (BAD-P), and BAX content under control and ADX conditions. The results derived from four or five independent experiments, were quantified by computerized densitometry and normalized with respect to the relative intensity of β-actin or total protein, as in the case of BAD (Fig. 4B). The contents of the anti-apoptotic protein BCL-2 and the pro-apoptotic BAX were similar to sham animals, indicating that the levels of these proteins did not change after long-term ADX, showing a correspondence with mRNA levels. In contrast,

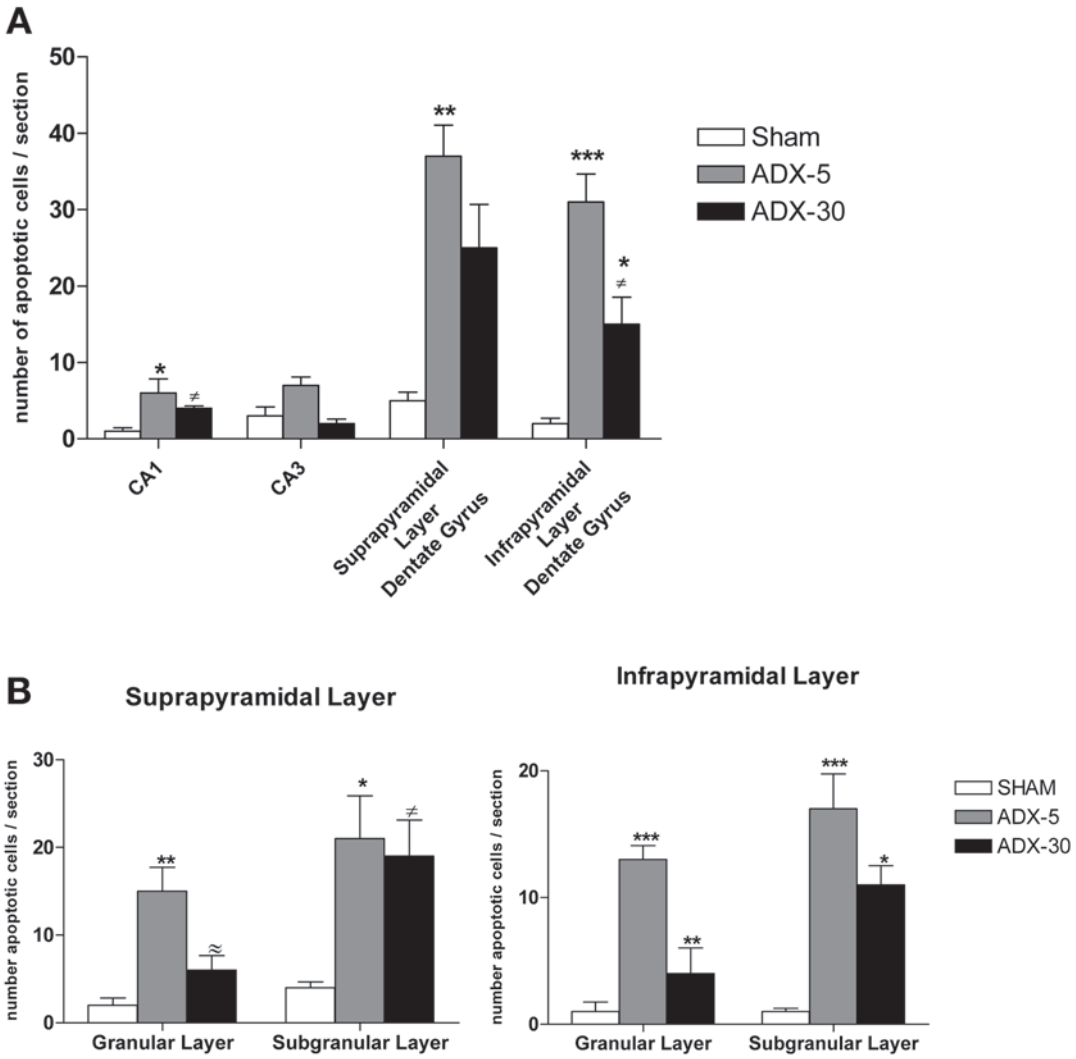

Fig. 1. Apoptotic morphology in the hippocampus after adrenalectomy. (**A**) Number of cells displaying morphological alterations in the GD and CA regions 5 and 30 d after ADX. Values indicate the mean value of the number of damaged cells present in five sections ± SEM from four or five animals. (**B**) Number of apoptotic cells present in granular layer and subgranular zone of DG. The results were analyzed by one-way ANOVA, followed by post-hoc Tukey test. *$p < 0.05$ vs sham; **$p < 0.01$ vs sham; ***$p < 0.001$ vs sham; $^{\neq}p < 0.05$ vs ADX-5; $^{\approx}p < 0.01$ vs ADX-5.

the BCL-X_L content in 30-d ADX rats increased 50% with respect to sham controls, a result that correlates with the increased level of *Bcl-x* mRNA. Figure 4B shows that long-term ADX results in the reduction of the pro-apoptotic BAD protein without changing its inactive phosphorylated form (Ser^{112}).

Discussion

The apoptotic response of GD neurons to ADX is highly complex and poorly understood. In the present study, we found that after long-term ADX there is (i) no change in the corticosterone levels with respect to short-term ADX, (ii) a reduction in the morphological alterations around the GD with features similar to apoptosis, (iii) a decrease in the levels of initiator caspase-9 in the entire hippocampus, (iv) a decrease in the pro-apoptotic protein BAD and no change in its inactive form (BAD-Ser^{112}), and (v) an increase in the anti-apoptotic *Bcl-x* mRNA, mainly in the suprapyramidal layer accompanied by a rise in whole hippocampal BCL-X_L protein.

Adrenalectomy Promotes Morphological Changes Associated with Hippocampal Apoptosis

An important observation of previous studies is that short-term ADX-induced apoptosis is restricted only in GD cells suggesting that neurons of the CA3–CA1 subfields do not require corticosterone to survive or, more likely, express molecules that protect them from ADX-induced apoptotic cell death. In this study, we demonstrate that long-term ADX does not change the already decreased levels of corticosterone but does promote an apoptosis restricted to the subgranular zone that represents cell death probably associated with progenitor cells, glia, and/or immature neurons *(11)*.

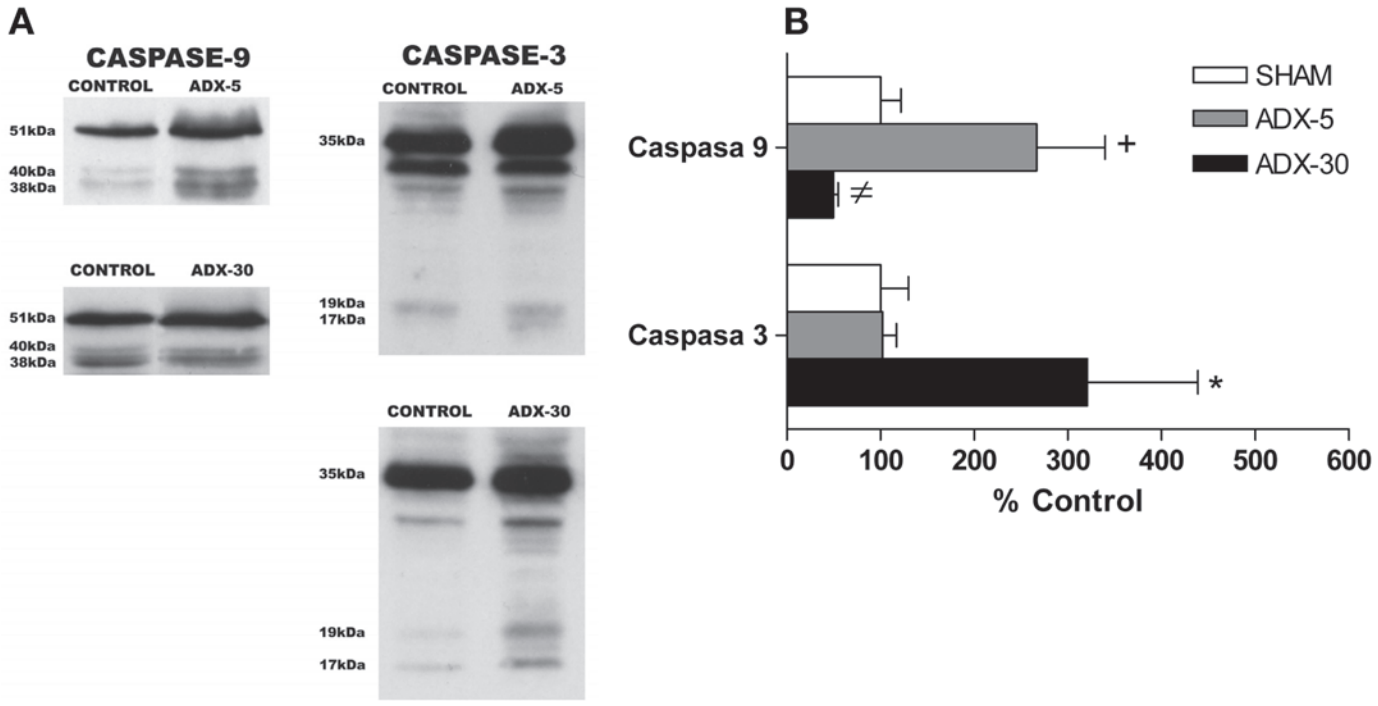

Fig. 2. Effects of long-term and short-term adrenalectomy on active caspase-9 and caspase-3 levels. Western blotting analysis of pro-caspase-3 and pro-caspase-9 and their cleaved fragments after ADX. (**A**) A representative immunoblot is shown. (**B**) Five days after ADX procaspase-9 processing is increased generating mainly the 38-kDa fragment. Thirty days after ADX caspase-3 processing, generating active caspase-3 (17 kDa) and the 19-kDa fragment, is elevated. The results were expressed as mean ± SEM and analyzed by one-way ANOVA, followed by post-hoc Tukey test. $^{+}p < 0.05$ vs sham; $^{\neq}p < 0.05$ ADX-5 vs ADX-30; $^{*}p < 0.05$ vs sham and vs ADX-5.

Also, we observed cell death in the mature granular DG cell layer; however, it occurred to a lesser extent compared to 5 d after ADX. It has been described that long-term ADX (months) does not promote entire DG cell loss, probably due to the presence of other sources that can supply sufficient steroids to prevent death in this region *(18)*. However, with our experimental conditions, the levels of hormone detected under ADX was similar after 5 d of ADX and significantly reduced compared to sham-control animals; thus, we can assume that long-term ADX induces different mechanisms that prevent cell death.

ADX and the mRNA Levels of Representative **Bcl-2** *Gene-Family Members*

Molecules related to the BCL-2 family are expressed normally in the CNS *(23,24)*. BCL-2, a repressor of apoptosis, is induced under neuronal insults to cells ordinarily resistant to apoptosis, indicating a protective role in mature neurons *(24–26)*. In contrast, BCL-X_L, with actions similar to BCL-2 *(21)*, is expressed in both embryonic *(27–29)* and adult neurons *(21,29,30)*, suggesting its participation in the control of apoptosis during development as well as the adult CNS *(31)*. Furthermore, BAX is normally expressed in the CNS *(25,32)* and is induced in several models of delayed neuronal cell death, acting as an apoptotic promoter *(25,26, 32–34)*. The cell death–inducing actions of this molecule can be antagonized by the presence of BCL-2 or BCL-X_L *(16, 35)*. BAD, another pro-apoptotic protein, binds strongly to BCL-X_L than BCL-2 in mammalian cells and prevents the death repressor activity of BCL-X_L, but not that of BCL-2 *(17,36)*. Also, the phosphorylation of BAD represents an important bridge between survival signaling by growth-factor receptors and the prevention of apoptosis *(37,38)*.

We previously demonstrated that 5 d after ADX there is an induction of the pro-apoptotic *Bax* mRNA and the anti-apoptotic *Bcl-2* mRNA in the DG *(10)*. In addition, changes were reported in gene expression in single dentate granule neurons after acute ADX *(39)*. In this study the Ca^{2+} current amplitude—a known risk factor for apoptosis—correlated negatively with *Bcl-2*/*Bax* mRNA expression *(39)*. Thus, cells with high BCL-2/BAX levels probably are protected against the apoptosis induced by short-term ADX.

In this paper we show that long-term ADX does not promote changes in *Bax* and *Bcl-2* mRNA levels in any hippocampal subfield, findings which correlate well with no variation in the protein content of whole hippocampal extracts (Fig. 4). We found, however, that the mRNA levels of the anti-apoptotic gene *Bcl-x* increased almost 100% in rats 30 d after ADX, mainly in the DG suprapyramidal layer, an effect accompanied by a 50% increase in the hippocampal content of BCL-X_L. This result suggests that long-term ADX promotes adaptative changes as a compensatory mechanism

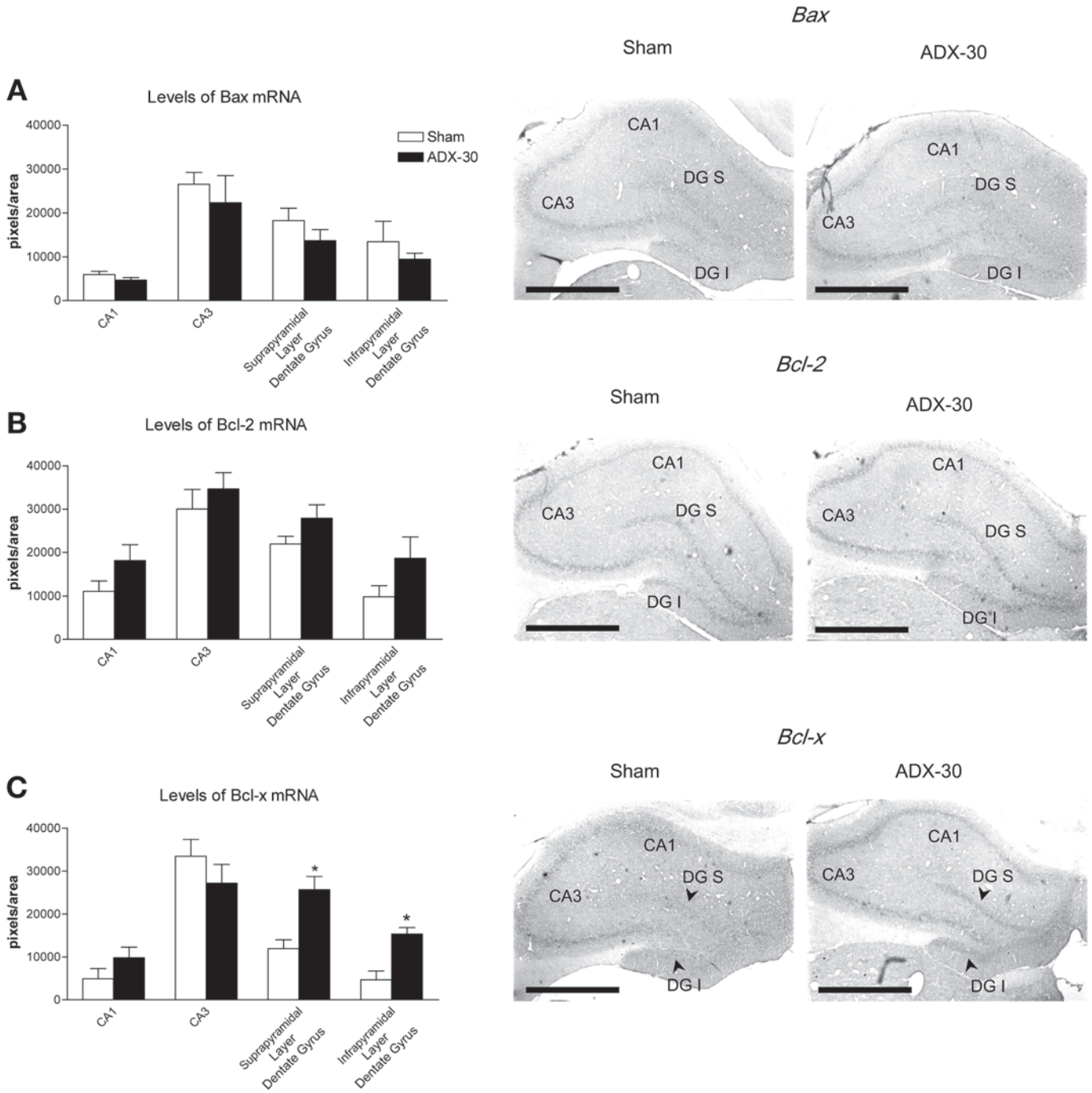

Fig. 3. Effect of ADX-30 on *Bax* mRNA, *Bcl-2* mRNA, and *Bcl-x* mRNA levels in hippocampus. Microphotographs illustrating the expression of *Bax* (**A**); *Bcl-2* (**B**) and *Bcl-x* (**C**) in the hippocampus of sham-operated 30 d after ADX. Scale bar = 1000 μm. Bar graph showing the semiquantitative analysis of ADX effect on mRNA levels in different neuronal cell layers [CA1, CA3, and suprapyramidal (DG S) and infrapyramidal (DG I) blades of DG], expressed as specific hybridization measured in pixels. Data are mean ± SEM. For comparison of the mean values between the two groups, statistical evaluation was done using the one-tailed Student's *t* test. *$p < 0.05$ vs sham.

to prevent apoptosis in the adult hippocampus. In agreement with this proposal, we did observe a reduction in the pro-apoptotic BAD protein in the hippocampus with no changes in phosphorylated Ser^{122}. It is well known that BAD promotes apoptosis through its heterodimerization with BCL-X_L in the mitochondrial membrane *(14)*. BAD phosphorylation at Ser^{122} and Ser^{136} creates binding sites for the phospho-specific binding of 14-3-3 proteins, which retain BAD in the cytoplasm, thus preventing the mitochondrial cytotoxic interaction with BCL-X_L *(17)*. However, Ser^{122} phos-

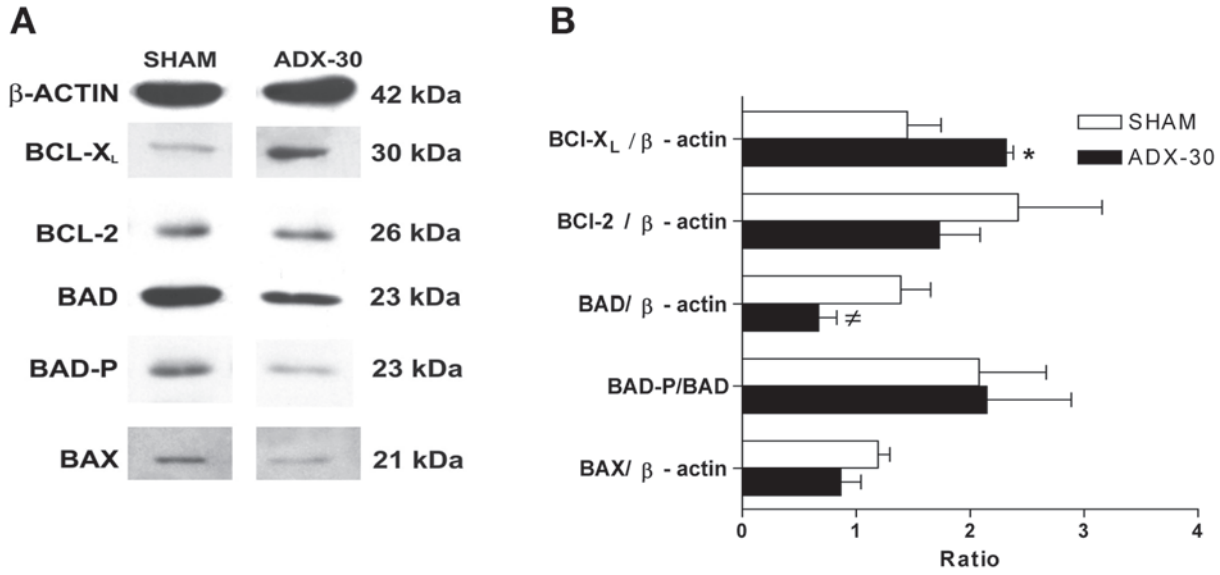

Fig. 4. (**A**) Representative immunoblot showing BCL-X_L, BCL-2, BAX, and BAD protein levels 30 d after ADX. Protein samples (50 μg protein/lane) were resolved by SDS-PAGE, and immunoblotting was performed with BCL-X_L, BCL-2, BAX, BAD, and phospho-BAD antibodies as described in Materials and Methods. (**B**) Relative intensity of protein bands from the immunoblots were measured as described in materials and methods. The data are shown as the mean ± SEM (n = 4–5). For comparison of the mean values between the two groups, statistical evaluation was done using the one-tailed Student's t test. *$p < 0.05$ vs sham; ≠$p < 0.05$ sham.

phorylation was shown to be absolutely required for the dissociation of BAD from BCL-X_L *(17)*. Recently it was reported that the phosphorylation of BAD at Ser^{155} also inhibits the death-promoting activity of BAD by interfering with its interaction with BCL-X_L *(40)*. Our results suggest that a reduction of corticosterone induces cell death and also activates mechanisms that protect against apoptosis.

Adrenalectomy, Caspase Activation, and Cell Death

Caspase-dependent, apoptotic programmed cell death is associated with proteolysis and disassembly of the cellular scaffolding *(19,41)*. Caspase, a family of cysteine proteases, exists as a group of inactive zymogens that possess a prodomain and a protease domain, which must be split to release the active form *(19,41)*. This event could be activated by either an extrinsic (activation of a death receptor) or intrinsic (mitochondrial or apoptosome) pathway *(14,19,41)*. Upon apoptotic stimulation the intrinsic pathway is activated by the mitochondrial release of pro-apoptotic factors or proteins such as cytochrome *c*, apoptotic inducing factor (AIF), and Smac/Diablo *(14,19,41)*. Cytochrome *c* released from mitochondria associates with procaspase-9 and Apaf 1 forming the apoptosome complex and promoting the proteolytic cleavage of executor caspases (e.g., caspase-3) *(14,19,41, 42)*. Caspase-9 active peptides in brain extracts are present during brain development and remain at extremely low levels in the adult brain *(43)*. In the present study we found an increase in the active peptide fragment of caspase-9 only 5 d after ADX, without any change in caspase-3 processing (Fig. 2B). The caspase-9 processing could be related to BAX induction observed under adrenalectomy *(10)* probably promoting cytochrome *c* release from mitochondria *(15–17)*. Thus, we suggest that cell death observed at this time is probably associated with the participation of other executor caspases such as 7 or 6 *(44)* (Fig. 5). Alternatively apoptosis observed 5 d after ADX could correspond to cell death promoted by caspase-independent mechanisms *(45)* (Fig. 5). Among them, the most common is associated to the release of AIF from mitochondria *(45,46)*. AIF is able to translocate to the nucleus producing DNA fragmentation and nuclear condensation *(46)*, giving account, perhaps to the morphological changes observed 5 d after ADX. In contrast, after long-term ADX we observed a reduction in the extent of apoptosis mainly in DG mature cells as compared with short-term ADX (Fig. 1B). Because the release of mitochondria-derived pro-apoptotic molecules occurs secondary to translocation of one or more members of the BCL-2 protein family, we hypothesize that an increase in BCL-X_L and the reduction in BAD accounts for apoptosis reduction in the DG mature layer after long-term ADX (Fig. 1). In contrast, the apoptosis that was observed is independent of caspase-9 and probably caspase-3 dependent, the latter being activated perhaps through the extrinsic pathway (caspase-8) *(15)* or through the participation of a calcium-dependent protease like calpain *(44,47,48)*. Interestingly, pro-caspase 3 is cleaved by calpain, related to the induction of a long-term ADX apoptotic program. In addition, calpain could promote apoptosis through caspase-12 processing *(49)*. Based on these data, a proposed model for apoptosis induced by long-term ADX is shown in the Fig. 5.

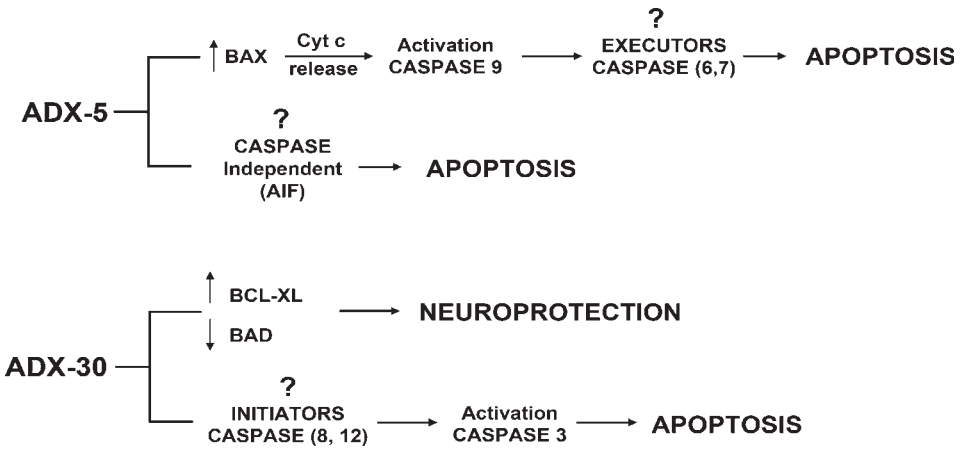

Fig. 5. Schematic representation of apoptotic pathway induced after short-term and long-term adrenalectomy.

Conclusion

Our results strongly suggest that the decrease in hippocampal cellular death found after long-term ADX could be related to both the induction of the anti-apoptotic protein BCL-X_L and the reduction in BAD, a pro-apoptotic member, changes that increase the chance for cellular survival. Also, the caspase-9 processing observed suggests that 5 d after ADX the apoptosis could be related to the mitochondrial pathway which is observed after long-term ADX could correspond to a mechanism related to the extrinsic pathway and/or through the participation of calpain which would account for the caspase-3 processing.

Materials and Methods

Animals

Adult male Sprague–Dawley rats (250–280 g), derived from a stock maintained at the University of Chile, were used. They were allowed free access to pelleted food, maintained with controlled temperature (22°C) and photoperiods (lights on from 0700 to 1900 h). All animal procedures were performed using protocols approved by the Institutional Ethical Committee of the Faculty of Chemical and Pharmaceutical Sciences, University of Chile.

Animal Surgery

Bilateral ADX was performed under fluothane anesthesia (1.5% v/v air) and the animals were maintained with 0.9% NaCl as their drinking solution. The sham-operated group of rats underwent skin and lumbar muscle incision, leaving the adrenal untouched.

Tissue Fixation

Sham-operated and ADX animals, 5 or 30 d after surgery were anesthetized and a blood sample was taken from the heart. They were then transcardiacally perfused with 100 mL of 0.9% NaCl followed by 500 mL of 4% paraformaldehyde in 0.1 *M* phosphate buffer pH 7.4 (PB). The brain was dissected from the skull, post-fixed in the same buffer overnight and then immersed in 30% sucrose in 0.1 *M* PBS (phosphate-buffered saline) at 4°C for 2 d. Coronal sections (14 μm thick) were sliced from the frozen fixed brains and processed for Nissl stain or for *in situ* hybridization.

Apoptotic Morphology

Sections were stained with 1% Cresyl Violet for 20 min, dehydrated in alcohol, and mounted in Entellan (Merck, Darmstadt, Germany). Apoptotic nuclei were localized using at a 100× magnification. Cells displaying small condensed nuclei, extensive and tight condensation of nuclear material into darkly stained balls and disassembly of the pyknotic cells into apoptotic bodies, were considered as apoptotic *(10)*. Cells bordering the subgranular zone and the granular zone were counted bilaterally. The data shown were obtained from four or five brain sections per animal.

In Situ *Hybridization*

Floating sections were incubated with cRNA probes transcribed with Sp6 polymerase (*Bcl-2* and *Bcl-x*) or T7 polymerase (*Bax*) using the Digoxigenin RNA labeling kit (Roche, Molecular Biochemicals, Mannheim, Germany) as previously described *(10)*. For semiquantitative analysis, densitometric measurements of each hippocampal subfield were analyzed using UN-SCAN-IT software (Silk Scientific Inc., Orem, UT, USA). The data were obtained as a gray scale value of the measured hippocampal areas, i.e., being the larger optical density value the darker staining and the lower value the lighter staining. The low hybridization signal in the stratum radiatum was considered as background, and this was subtracted from the optical density values for the hippocampal cell layers. Data are expressed as optical density (pixels) and for each animal the value represents the average of measurements from four or five brain sections.

Western Blotting Analysis

In a separate, but similarly treated group of animals, hippocampi were dissected, homogenized, and subjected to

immunoblot analysis as previously described *(9)*. For an evaluation of caspase activation, the membranes were incubated with a rabbit polyclonal antibody raised against procaspase-3 (35 kDa) and fragments of the cleaved caspase-3 (19 and 17 kDa) (1:1000 dilution, Cell Signaling, MA, USA) or with a rabbit polyclonal antibody that recognizes the full-length procaspase-9 (51 kDa) and fragments of the cleaved procaspase-9 (40, 38, and 17 kDa) at a working dilution of 1:1000 (Cell Signaling, MA, USA) in a saline phosphate buffer containing 0.1 % Tween-20 (TPBS). The membranes were incubated overnight with the primary antibody, then washed and incubated with a peroxidase conjugated secondary antibody for 2 h. After additional washes, the membranes were incubated with an enhanced chemiluminescent substrate, according to the manufacturer's instructions (Perkin Elmer Life Sciences, Boston, MA) and exposed to X-ray film (MR-1 Eastman-Kodak, Rochester, NY). The intensity of the bands was determined and analyzed using the UN-SCAN-IT program and results are expressed as the ratio between the active caspase band intensity vs the pro-caspase band; values are normalized with respect to controls.

For evaluation of the changes in the pro- and anti-apoptotic proteins related to the *Bcl-2* gene family (BAX, BCL-2, and BCL-X_L), these changes were measured as we described previously *(9)*. Immunodetection of phospho-BAD and total BAD (Cell Signaling, MA, USA) was accoplished in 3% nonfat dry milk-TPBS in a 1:1000 working solution. As a control for the amount of protein loaded in each lane, the membranes were stripped with ponceau red and reprobed for β-actin content (Sigma, St Louis, MO, USA). The intensity of each band was measured as above, and the results are expressed as a ratio to the β-actin or total BAD, in the case of phospho-BAD.

Corticosterone Radio Immunoassay

Corticosterone levels were determined by RIA as per the manufacturer's instructions (Sigma, St. Louis, MO, USA), and as described previously, on diluted serum samples *(9)*.

Statistical Analysis

To determine the effect of ADX on serum corticosterone levels, apoptosis (Fig. 1), and caspase levels (Fig. 2), data were analyzed by ANOVA tests with a Tukey post-hoc test. To find out changes in gene expression (Fig. 3) and protein levels (Fig. 4) we used one-tail *t*-test. The level of significance was set at $p \leq 0.05$. The statistical analysis was carried out with GraphPad Prism 4.0 (GraphPad Software, San Diego, CA).

Acknowledgments

This research was supported by Proyecto de Enlace Facultad, Memorias 2000-2003, CEPEDEQ 2003 grants (to Fiedler JL.) and B-010-0312 (to Parra C.).

References

1. De Kloet, E. R., Vreugdenhil, E., Oitzl, M. S., and Joels, M. (1998). *Endocr. Rev.* **19,** 269–301.
2. Datson, N. A., van der Perk, J., de Kloet, E. R., and Vreugdenhil, E. (2001). *Eur. J. Neurosci.* **14,** 675–689.
3. Abraham, I. M., Harkany, T., Horvath, K. M., and Luiten, P. G. (2001). *J. Neuroendocrinol.* **13,** 749–760.
4. Small, S. A. (2002). *Rev. Neurosci.* **13,** 183–194.
5. Sloviter, R. S., Valiquette, G., Abrams, G. M., et al. (1989). *Science* **243,** 535–538.
6. Sloviter, R. S., Sollas, A. L., Dean, E., and Neubort, S. (1993). *J. Comp. Neurol.* **330,** 324–336.
7. Sloviter, R. S., Dean, E., and Neubort, S. (1993). *J. Comp. Neurol.* **330,** 337–351.
8. Woolley, C. S., Gould, E., Sakai, R. R., Spencer, R. L., and McEwen, B. S. (1991). *Brain Res.* **554,** 312–315.
9. Greiner, M., Cardenas, S., Parra, C., et al. (2001). *Endocrine* **15,** 323–333.
10. Cardenas, S. P., Parra, C., Bravo, J., et al. (2002). *Neurosci. Lett.* **331,** 9–12.
11. Cameron, H. A. and Gould, E. (1996). *J. Comp. Neurol.* **369,** 56–63.
12. Cameron, H. A., Tanapat, P., and Gould, E. (1998). *Neuroscience* **82,** 349–354.
13. Gould, E. (1994). *Ann. NY Acad. Sci.* **743,** 73–92; discussion 92–93.
14. Kuwana, T. and Newmeyer, D. D. (2003). *Curr. Opin. Cell. Biol.* **15,** 691–699.
15. Hengartner, M. O. (2000). *Nature* **407,** 770–776.
16. Oltvai, Z. N., Milliman, C. L., and Korsmeyer, S. J. (1993). *Cell* **74,** 609–619.
17. Zha, J., Harada, H., Yang, E., Jockel, J., and Korsmeyer, S. J. (1996). *Cell* **87,** 619–628.
18. Conrad, C. D. and Roy, E. J. (1993). *J. Neurosci.* **13,** 2582–2590.
19. Chang, H. Y. and Yang, X. (2000). *Microbiol. Mol. Biol. Rev.* **64,** 821–846.
20. Stennicke, H. R. and Salvesen, G. S. (2000). *Biochim. Biophys. Acta* **1477,** 299–306.
21. Boise, L. H., Gonzalez-Garcia, M., Postema, C. E., et al. (1993). *Cell* **74,** 597–608.
22. Tilly, J. L., Tilly, K. I., Kenton, M. L., and Johnson, A. L. (1995). *Endocrinology* **136,** 232–241.
23. Abe-Dohmae, S., Harada, N., Yamada, K., and Tanaka, R. (1993). *Biochem. Biophys. Res. Commun.* **191,** 915–921.
24. Merry, D. E. and Korsmeyer, S. J. (1997). *Annu. Rev. Neurosci.* **20,** 245–267.
25. Krajewski, S., Mai, J. K., Krajewska, M., Sikorska, M., Mossakowski, M. J., and Reed, J. C. (1995). *J. Neurosci.* **15,** 6364–6376.
26. Chen, J., Zhu, R. L., Nakayama, M., et al. (1996). *J. Neurochem.* **67,** 64–71.
27. Gonzalez-Garcia, M., Perez-Ballestero, R., Ding, L., et al. (1994). *Development* **120,** 3033–3042.
28. Motoyama, N., Wang, F., Roth, K. A., et al. (1995). *Science* **267,** 1506–1510.
29. Mizuguchi, M., Sohma, O., Takashima, S., et al. (1996). *Brain Res.* **712,** 281–286.
30. Parsadanian, A. S., Cheng, Y., Keller-Peck, C. R., Holtzman, D. M., and Snider, W. D. (1998). *J. Neurosci.* **18,** 1009–1019.
31. Gonzalez-Garcia, M., Garcia, I., Ding, L., et al. (1995). *Proc. Natl. Acad. Sci. USA* **92,** 4304–4308.
32. Xiang, H., Kinoshita, Y., Knudson, C. M., Korsmeyer, S. J., Schwartzkroin, P. A., and Morrison, R. S. (1998). *J. Neurosci.* **18,** 1363–1373.
33. Blum, D., Wu, Y., Nissou, M. F., Arnaud, S., Alim Louis, B., and Verna, J. M. (1997). *Brain Res.* **751,** 139–142.
34. Johnson, M. D., Xiang, H., London, S., et al. (1998). *J. Neurosci. Res.* **54,** 721–733.

35. Yin, X. M., Oltvai, Z. N., and Korsmeyer, S. J. (1994). *Nature* **369,** 321–323.
36. Yang, E., Zha, J., Jockel, J., Boise, L. H., Thompson, C. B., and Korsmeyer, S. J. (1995). *Cell* **80,** 285–291.
37. Scheid, M. P., Schubert, K. M., and Duronio, V. (1999). *J. Biol. Chem.* **274,** 31108–31113.
38. Zhu, Y., Ahlemeyer, B., Bauerbach, E., and Krieglstein, J. (2001). *Neurochem. Int.* **38,** 227–235.
39. Qin, Y., Nair, S., Karst, H., Vreugdenhil, E., Datson, N., and Joels, M. (2003). *Brain Res. Mol. Brain Res.* **111,** 17–23.
40. Tan, Y., Demeter, M. R., Ruan, H., and Comb, M. J. (2000). *J. Biol. Chem.* **275,** 25865–25869.
41. Boatright, K. M. and Salvesen, G. S. (2003). *Curr. Opin. Cell Biol.* **15,** 725–731.
42. Stefanis, L. (2005). *Neuroscientist* **11,** 50–62.
43. Cao, G., Luo, Y., Nagayama, T., et al. (2002). *J. Cereb. Blood Flow Metab.* **22,** 534–546.
44. Rami, A. (2003). *Neurobiol. Dis.* **13,** 75–88.
45. Assuncao Guimaraes, C. and Linden, R. (2004). *Eur. J. Biochem.* **271,** 1638–1650.
46. Hong, S. J., Dawson, T. M., and Dawson, V. L. (2004). *Trends Pharmacol. Sci.* **25,** 259–264.
47. McGinnis, K. M., Gnegy, M. E., Park, Y. H., Mukerjee, N., and Wang, K. K. (1999). *Biochem. Biophys. Res. Commun.* **263,** 94–99.
48. Wang, K. K. (2000). *Trends Neurosci.* **23,** 20–26.
49. Sergeev, I. N. (2004). *Biochem. Biophys. Res. Commun.* **321,** 462–467.